Optical patient interface in femtosecond laser–assisted cataract surgery: Contact corneal applanation versus liquid immersion

Jonathan H. Talamo, MD, Philip Gooding, MS, David Angeley, MS, William W. Culbertson, MD, Georg Schuele, PhD, Daniel Andersen, BS, George Marcellino, PhD, Emma Essock-Burns, PhD, Juan Batlle, MD, Rafael Feliz, MD, Neil J. Friedman, MD, Daniel Palanker, PhD

PURPOSE: To compare 2 optical patient interface designs used for femtosecond laser–assisted cataract surgery.

SETTING: Optimedica Corp., Santa Clara, California, USA, and Centro Laser, Santo Domingo, Dominican Republic.

DESIGN: Experimental and clinical studies.

METHODS: Laser capsulotomy was performed during cataract surgery with a curved contact lens interface (CCL) or a liquid optical immersion interface (LOI). The presence of corneal folds, incomplete capsulotomy, subconjunctival hemorrhage, and eye movement during laser treatment were analyzed using video and optical coherence tomography. The induced rise of intraocular pressure (IOP) was measured in porcine and cadaver eyes.

RESULTS: Corneal folds were identified in 70% of the CCL cohort; 63% of these had areas of incomplete capsulotomies beneath the corneal folds. No corneal folds or incomplete capsulotomies were identified in the LOI cohort. The mean eye movement during capsulotomy creation (1.5 sec) was 50 μm with a CCL and 20 μm with an LOI. The LOI cohort had 36% less subconjunctival hemorrhage than the CCL cohort. During suction, the mean IOP rise was 32.4 mm Hg ± 3.4 (SD) in the CCL group and 17.7 ± 2.1 mm Hg in the LOI group.

CONCLUSIONS: Curved contact interfaces create corneal folds that can lead to incomplete capsulotomy during laser cataract surgery. A liquid interface eliminated corneal folds, improved globe stability, reduced subconjunctival hemorrhage, and lowered IOP rise.

Financial Disclosure: Drs. Talamo, Culbertson, Batlle, Feliz, and Palanker are consultants to and Messrs. Gooding, Angeley, Schuele, Marcellino, and Andersen, and Ms. Essock-Burns are employees of Optimedica Corp., Sunnyvale, California, USA.

J Cataract Refract Surg 2013; ■:■–■ © *2013 ASCRS and ESCRS*

Proper delivery of laser energy into the eye for surgical procedures requires an optomechanical interface that serves 2 functions: (1) optical coupling to allow efficient delivery of the laser beam into the transparent ocular tissues and (2) maintaining mechanical stability of the eye during laser application. For image-guided procedures such as femtosecond laser–assisted cataract surgery, this interface performs a third function; that is, permitting accurate acquisition of 2- and 3-dimensional (3-D) images of ocular anatomy that are coregistered with the therapeutic laser system to guide the treatment.

A common optomechanical ocular interface design uses corneal applanation, as in laser in situ keratomileusis (LASIK). With this approach, a flat transparent window is pressed against the cornea using a suction ring applied just outside the limbus.[1] A flat glass contact surface is used as an optical and mechanical reference for flap thickness, eliminating the need for 3-D eye tracking to guide the laser focus. Strong deformation of the eye during applanation typically results in significant elevation of the intraocular pressure (IOP)—up to 90 mm Hg above baseline values.[2–4] This level of pressure rise can restrict retinal blood flow, which poses a risk for optic nerve damage and/or retinal vascular occlusion.[5] This is of particular concern in an elderly patient population and in some

0886-3350/$ - see front matter
http://dx.doi.org/10.1016/j.jcrs.2013.01.021

individuals with glaucoma. In addition, such strong suction often results in large areas of bulbar subconjunctival hemorrhage.[6]

A contact lens with a curved surface that approximates the natural radius of curvature of the anterior cornea reduces globe deformation and associated IOP rise when compared with a flat contact lens. However, because the diameter and curvature of the cornea vary appreciably from patient to patient, 1 standard curved interface cannot perfectly match every patient's eye. Alternatively, matching individual corneas from a selection of variable curved contact lenses is process intensive and not economical. Pressing the cornea against a rigid surface with a curvature different from the cornea's natural shape causes deformations of the cornea; ie, unwanted folds in the posterior surface. Such folds in the posterior corneal surface do not affect the laser focusing inside the stroma; therefore, this effect is not a significant issue in the corneal flap cutting during LASIK refractive surgery. However, for the beam focused several millimeters posterior to the cornea, the effect of the corneal folds is critically important.

A liquid immersion interface is an alternative solution for reducing eye deformation and the associated IOP rise. A layer of transparent fluid between the cornea and an optical window provides a clear path for the laser beam and allows imaging of high optical quality. Mechanical attachment in this case is achieved with a suction ring outside the limbus. Anatomic variation is minimal in this region of contact, thus minimizing globe deformation and patient-to-patient variation using 1 standard attachment. Because the cornea itself is in contact with liquid rather than a rigid surface, it is not forced to conform to a different shape. Therefore the liquid interface does not induce corneal folds.

In this study, we compared a curved contact lens interface (CCL) with a liquid optical immersion interface (LOI) for the creation of femtosecond laser capsulotomies. The performance of each type of optomechanical interface was evaluated in patients by assessing the presence of corneal folds, completeness of anterior capsulotomies, mechanical stability of the eye, and the amount of subconjunctival hemorrhage produced. The IOP rise was assessed in vitro using porcine and cadaver eyes attached to the same devices.

Submitted: September 26, 2012.
Final revision submitted: January 14, 2013.
Accepted: January 15, 2013.

From Talamo Hatch Laser Eye Consultants (Talamo), Waltham, Massachusetts, Optimedica Corp. (Gooding, Angeley, Schuele, Andersen, Marcellino, Essock-Burns), Santa Clara, Mid-Peninsula Ophthalmology Medical Group (Friedman), Palo Alto, and Department of Ophthalmology (Friedman, Palanker), Stanford University, Stanford, California, Bascom Palmer Eye Institute (Culbertson), University of Miami Miller School of Medicine, Miami, Florida, USA; Centro Laser, Santo Domingo (Batlle, Feliz), Dominican Republic.

Corresponding author: Jonathan H. Talamo, MD, Talamo Hatch Laser Eye Consultants, 1601 Trapelo Road, Suite 184, Waltham, Massachusetts 02451, USA. E-mail: jtalamo@lasikofboston.com.

MATERIALS AND METHODS

Laser System

The laser system for cataract surgery has been described in detail.[7,8] The same prototype laser system was used in all the studies described in this article and can be summarized briefly as follows: It includes a 3-D scanning femtosecond laser (1.03 μm wavelength, 400 femtosecond pulse duration, up to 10 μJ pulse energy, up to 120 kHz repetition rate). The femtosecond laser is coregistered throughout the volume of the ocular anterior segment with a spectral-domain optical coherence tomography (OCT) system configured with an equivalent 10 μm depth resolution and an axial range over 15.0 mm in water as well as a fixed-focus near-infrared video imaging. The OCT and video provide lateral identification and axial ranging of the target tissues throughout the anterior part of the eye that includes the cornea, limbus, the iris, and the lens. The system allows 3-D mapping of the cornea and lens with the OCT and video and creates laser treatment patterns based on these data. The laser scanner then precisely delivers the selected patterns to the target structures. Typical spot spacing for the laser patterns ranges from 5 to 20 μm laterally and 10 to 30 μm axially, depending on the desired effect.

The laser system video uses monochromatic, polarized, near-infrared (735 nm) illumination. A large depth-of-focus dark field–illuminated telecentric imaging system is focused on the iris. The imaging sensor is cross-polarized with respect to the incident light. This helps eliminate specular reflections of the illuminating light and thereby better uses the more informative back-scattering signals.

Curved Contact Lens and Liquid Optical Immersion Interfaces

Figure 1, *A*, is a simplified diagram of the patient interface with a CCL interface. Due to difficulties matching the complex anterior eye shape, including the cornea, limbus, and sclera, to a lens with a single radius of curvature, the clear aperture for the lens was limited to 10.8 mm in diameter. The concave radius of curvature for the lens surface in contact with the cornea was 8.3 mm, a little flatter than the nominal 7.8 mm radius for the anterior cornea. It was chosen so the cornea would first come in contact with the lens at the center to minimize potential problems caused by a residual air pocket. The material for the lens, its thickness, and the radius were chosen to optimize optical performance for both imaging and laser energy delivery inside the eye. Using a motorized bed and user control, the patient's eye was aligned with the optical system under direct real-time video monitoring. Final placement and docking of the eye to the CCL interface is achieved using suction.

Figure 1, *B*, shows the patient interface using liquid immersion. The LOI module comprises 2 parts. First, a plastic cup with a suction ring is placed on the patient's eye and suction is applied to hold it in place. Figure 2 shows how the cup is filled with a balanced salt solution before docking with the laser system. The second part includes the disposable

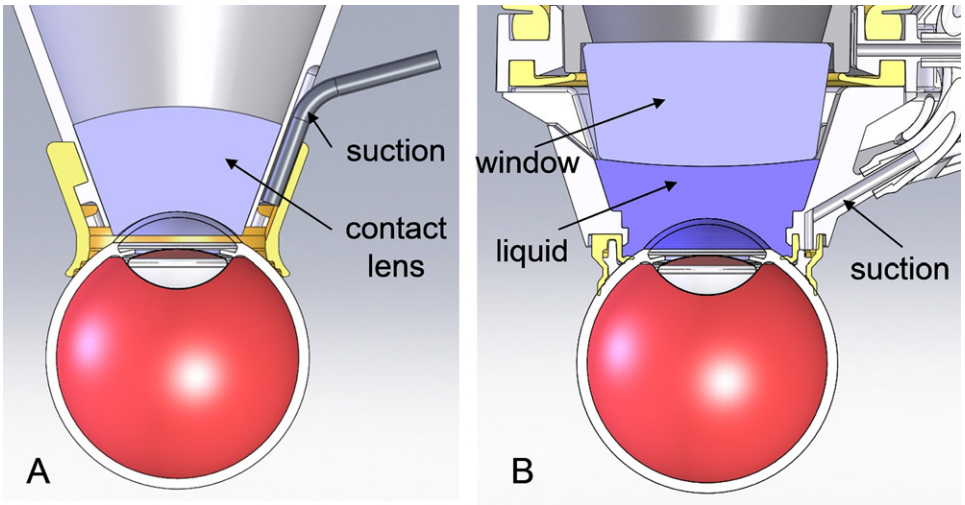

Figure 1. The optomechanical interfaces of the laser system with a patient's eye. *A*: Curved contact lens interface. *B*: Liquid optical immersion interface.

window attached to the laser system. The patient is elevated on a motorized bed to dock the plastic cup filled with balanced salt solution to the window. The transparent window is immersed so that the gap between the glass and the cornea is completely filled with liquid.

The LOI conforms to the complex shape of the corneal and limbal surfaces of any eye; thus, the clear aperture at the cornea anterior surface can be extended to 14.5 mm. This allows unobstructed viewing of the limbus during patient alignment and docking as well as subsequent imaging and laser treatment. Transparent liquid (eg, balanced salt solution) fills the gap with a nominal axial distance of 4.0 mm between the cornea and the transparent window that connects to the laser's internal optical system. The liquid's index of refraction closely matches that of the cornea, thereby largely nullifying its refractive effects. In addition, the liquid interface removes the optical constraints imposed by the CCL interface. As such, the refractive index and glass thickness of the window lens can be adjusted to optimize optical performance. In these studies, the liquid interface and window parameters were designed so that both the CCL and LOI configurations could be exchanged without unduly affecting optical parameters such as telecentricity, numerical aperture, and aberration correction. Focal shifts and lateral scaling were calibrated and applied separately for each configuration. The distal surface of the optical window was made convex to minimize occurrences of trapping air bubbles.

Figure 2. The LOI interface is composed of 2 pieces. A suction ring with a plastic cup is first attached to the patient's eye. The cup is then filled with a balanced salt solution before it is locked to the disposable laser output window lens.

In Vivo Human Study

All surgeries were performed at the Centro Laser, Santo Domingo, Dominican Republic, after institutional review board approval of the study protocol for laser-assisted cataract surgery was obtained from the Dominican Republic independent review board (Conabios, Santo Domingo, Dominican Republic). Informed consent was obtained from all participants. Laser-assisted cataract surgery was performed in 1 eye while the fellow eye served as a control for manual cataract surgery.

Patients were eligible for the study if they had grade 1 to 4 nuclear sclerotic cataracts according to the Lens Opacities Classification System III (LOCS III),[9] understood the informed consent document, and were able to comply with the treatment and follow-up schedule. Additional inclusion criteria were corrected distance visual acuity worse than 20/30, pupil dilation of at least 7.0 mm, and axial length of the eye between 22.0 mm and 26.0 mm. Exclusion criteria included enrollment in another drug or device study within the previous 3 months, an anterior chamber depth less than 2.5 mm, and corneal astigmatism greater than 5.0 diopters. Additional contraindications were a history of ocular trauma, coexisting ocular disease affecting vision, or previous ocular surgery (except previous cataract surgery in the fellow eye). The patients ranged from 55 to 80 years of age; 58 (60%) were women and 39 (40%) men. The full range of nuclear sclerotic lens grades (1 to 4) were treated; however, more than 50% of patients had LOCS III grade 3 or 4 cataract.

All eyes were dilated before surgery with 1 drop each of cyclopentolate 1.00% and phenylephrine 2.50% (3 doses at 20-minute intervals) and scopolamine 0.25% (2 doses at 20-minute intervals) starting 1 hour before the laser procedure. One drop of flurbiprofen 0.03% was also administered 40 minutes before surgery, and a Honan balloon was applied to the eye for the final 10 to 15 minutes before the laser treatment was initiated. Eyes were docked to the laser using a CCL or LOI as described above. No eyelid speculum or drapes were used.

After administration of a topical anesthetic agent (1 drop of proparacaine hydrochloride 0.5%), the laser system was

attached to the eye using a single-piece CCL interface or the 2-piece LOI by applying suction. Once the laser system was coupled to the eye through docking, OCT imaging was used to obtain a 3-D map of the patient's anterior segment anatomy; simultaneous near-infrared video provided a live image of the eye and lateral position guidance. The image-processing software automatically identified the anterior and posterior corneal surfaces, iris, and anterior and posterior lens surfaces. The prospective capsulotomy and lens fragmentation patterns based on the OCT data were displayed on a graphic user interface (GUI) for the surgeon's review. The superimposed video enables the surgeon to verify lateral positioning of the proposed laser treatment patterns. The GUI allows control over aspects of the laser cuts, such as *x-y-z* (axial) positioning, spot spacing, pattern shape, pattern size, and laser energy.

The capsulotomy pattern is a posterior-to-anterior spiral, starting in the lens tissue and terminating in the anterior chamber to ensure intersection of the incision with the anterior lens capsule. Advancing the focal spot in the anterior direction prevents scattering of the laser beam before its focal point on microbubbles and cracks in lens material that were formed in the previously treated locations. Instead, the bubbles and tissue cracks located below the current laser focus scatter the laser beam propagating beyond the focal spot and decrease the amount of laser radiation reaching adjacent structures, such as the iris, vitreous, and retina. The laser capsulotomy was completed in approximately 1.5 to 2.5 seconds using the following treatment parameters: 3 to 6 µJ pulse energy, 5 µm lateral spot spacing, 10 µm axial spacing, and 400 µm axial span of the capsulotomy pattern. The same range of laser pulse energies was used for capsulotomy creation with both types of patient interface. After the laser treatments were completed, the patients were transferred to a sterile operating room for phacoemulsification and implantation of a foldable intraocular lens with a 6.0 mm optic (Acrysof IQ SN60WF, Alcon/Novartis).

Corneal Folds and Incomplete Capsulotomies

The laser system video recordings and corneal OCT cross-sections obtained during the clinical trial were reviewed to identify the presence of corneal folds during 97 clinical procedures (n = 54 for CCL, n = 39 for LOI). Corneal folds manifest on OCT images as bumps on the posterior corneal surface (Figure 3, *A*), whereas they are visible within video images as faint gray lines brighter than the background (Figure 4, *A*). Corneal birefringence is altered by corneal folds, which makes them visible with cross-polarized infrared video imaging. Because corneal folds are on the cornea while the camera is focused on the iris, the folds are not ideally in focus.

Video images of laser capsulotomies were used to assess the location of corneal folds, the continuity of the capsulotomy incision, and the relationship between corneal folds and any observed incomplete capsulotomies. The OCT images were analyzed to confirm the presence of corneal folds identified on video images and to better characterize the anatomy of the corneal fold.

Optical Effects of Corneal Folds

The optical effect of corneal folds was modeled using optical analysis software (OSLO, Lambda Research Corp). The analysis was based on the observation of the pupil edge. It was noticed that this boundary of the iris appears discontinuous in the areas overlapping with the light gray lines

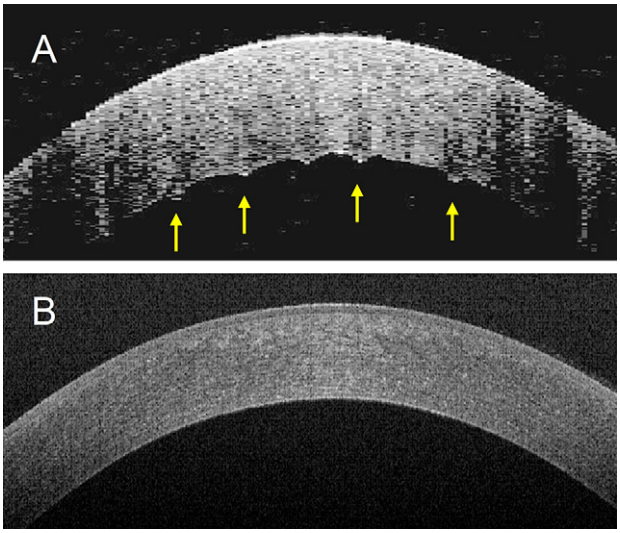

Figure 3. *A*: Typical OCT appearance of a cornea attached to the CCL. Folds are present on the posterior corneal surface (*arrows*). *B*: Typical OCT appearance of a cornea attached to the LOI. No folds are present.

corresponding to the corneal folds. The image shift of the pupil boundary under the folds seen in the video frames was measured and the effect modeled as a wedge inserted into the optical path. Analysis of the corneal OCT images was used as a basis for anatomic modeling of the corneal folds, while their optical effects were assessed using the optical modeling software (n = 54 for CCL, n = 39 for LOI).

Measurement of Intraocular Pressure Ex Vivo in Porcine and Human Cadaver Eyes

The IOP rise after docking was evaluated using a 20-gauge hypodermic needle attached to a MEMS fiber-optic remote pressure sensor (LIS-P1-N-62SC and OPP-M400-X-62SC-3.0PTFE-XN-60PK6-P1, Opense, Inc.) in freshly enucleated porcine (CCL n = 6; LOI n = 3) and human (LOI n = 3) cadaver eyes attached to the CCL or the LOI. The needle was inserted through the pars plana into the vitreous cavity before the laser system was docked.

Measurements of Eye Stability

To assess eye stability with both types of interfaces, near infrared (NIR) video recordings of the laser procedure were analyzed. Eye movements relative to the optical system were measured by monitoring the position of a unique fiduciary point selected in the image. Typically, a distinct area on the iris was selected for this purpose and then monitored during time intervals that were deemed critical phases of imaging and laser treatment: 1.5 seconds during capsulotomy, 20 seconds during lens fragmentation, and 2 minutes of the total docking time. The maximum movements of the fiduciary points over the sliding time windows of 1.5 seconds, 20 seconds, and 2 minutes were recorded for the full treatment duration in each included patient. The recorded values were sorted by magnitude, and the 95% probability point (P_{95}) was selected for each time interval. With that, 95% of the eye movements at any given time interval were smaller than P_{95}. Overall, 32 patients with the CCL and 24 patients with the LOI were analyzed.

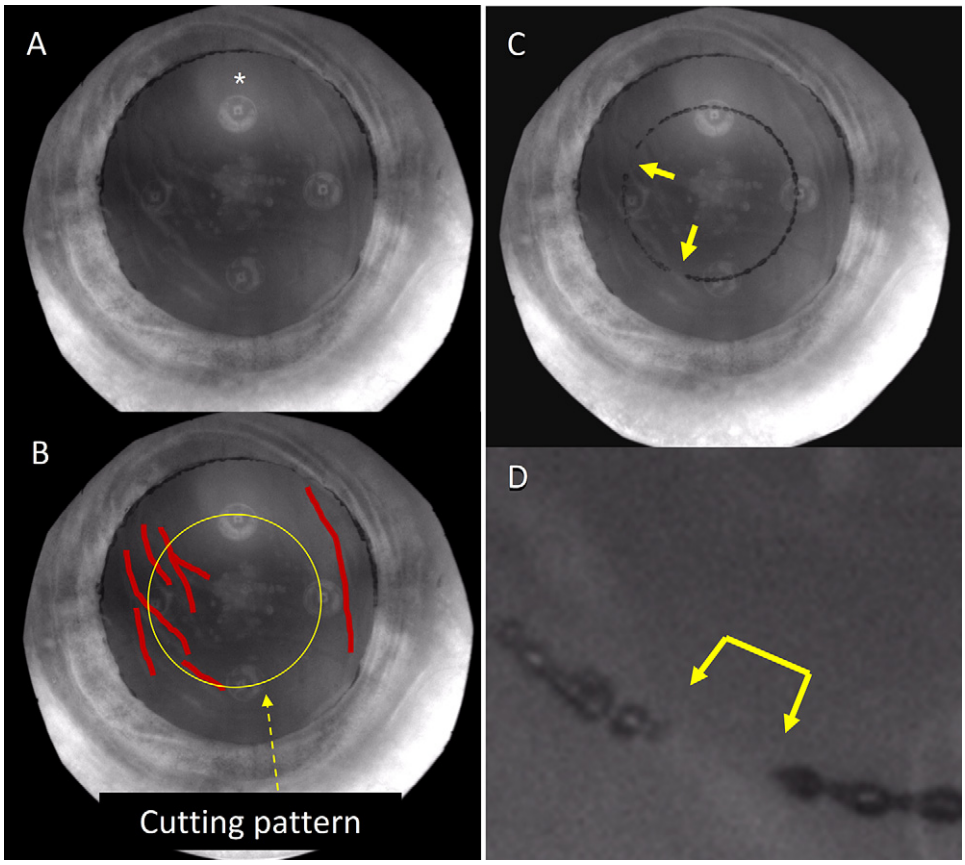

Figure 4. *A*: View of an eye attached to the CCL captured by the NIR video system. The 4 round spots at 12 (*asterisk*), 3, 6, and 9 o'clock are reflections of the illuminating near-infrared light-emitting diodes. *B*: The same image, with the corneal folds outlined by *red* lines. The capsulotomy cutting pattern is shown by a *yellow* ring. *C*: View of the eye after laser cutting. The gas microbubbles delineate the line of cutting, with gaps corresponding to positions of the corneal folds as indicated by the *red* ovals. *D*: Higher magnification of the capsulotomy incision with a gap near 7 o'clock, corresponding to the intersection of the laser treatment beam with an overlying corneal fold.

Measurements of Subconjunctival Hemorrhage

Suction rings are known to produce subconjunctival hemorrhage in patients having LASIK.[10] Proper design of the optomechanical interface should minimize this undesirable side effect. To quantify the extent of subconjunctival hemorrhage, the areas of bleeding were measured in the post-laser image of the eye. Images were acquired using a color camera (Figure 5, *A*), the region of interest on bulbar conjunctiva was identified by manual tracing visible sclera and limbus (Figure 5, *B*), and the total number of pixels in the outlined area were calculated. The image was then filtered by color to produce a binary map discriminating the bright red from the white background, as shown in Figure 5, *C*. The selected area of bleeding in the image after applying the threshold is shown as white. The ratio of the area of bleeding (measured as the number of pixels) to the total area of the sclera visible in the image was then compared for every patient. Thirty-six eyes were analyzed in this manner for the CCL and 35 eyes for the LOI.

RESULTS

Corneal Folds and Incomplete Capsulotomies

Of the 54 eyes treated with the CCL interface, 38 (70%) had observable corneal folds (Figure 3, *A*, and Figure 4, *A*). Corneal folds are highlighted in red in Figure 4, *B*, and the capsulotomy cutting pattern is shown in yellow. Figure 4, *C* and *D*, show the appearance of the laser cut with trapped microbubbles in the capsule, with incomplete incision areas directly below the corneal folds. Of 38 eyes with corneal folds, incomplete capsulotomies were observed in 24 cases (63%) or 44% of the total number of eyes treated with a CCL interface.

In the LOI treatment group, none of the 43 treated eyes had observable corneal folds and no incomplete capsulotomies were observed with video image analysis. The typical OCT appearance of the cornea under LOI is shown in Figure 3, *B*. A representative video frame of the laser capsulotomy performed with a LOI is shown in Figure 6, *A*. A close-up of the capsule cut is shown in Figure 6, *B*.

Optical Effects of Corneal Folds

The image of the pupil boundary under the folds was found to shift in the video frames by about 100 µm at the iris plane. The effect was modeled as a wedge inserted into the optical path. The wedge angle that would cause 100 µm displacement of an image positioned 4.0 mm from the cornea is 38 degrees. The OCT images further confirmed that the 38-degree wedge on the posterior cornea surface matched the anatomic appearance, as shown in Figure 7, *A*. In addition to the lateral shift of the laser focus by approximately 100 µm, the wedge significantly degraded the beam compared with the nominal optical

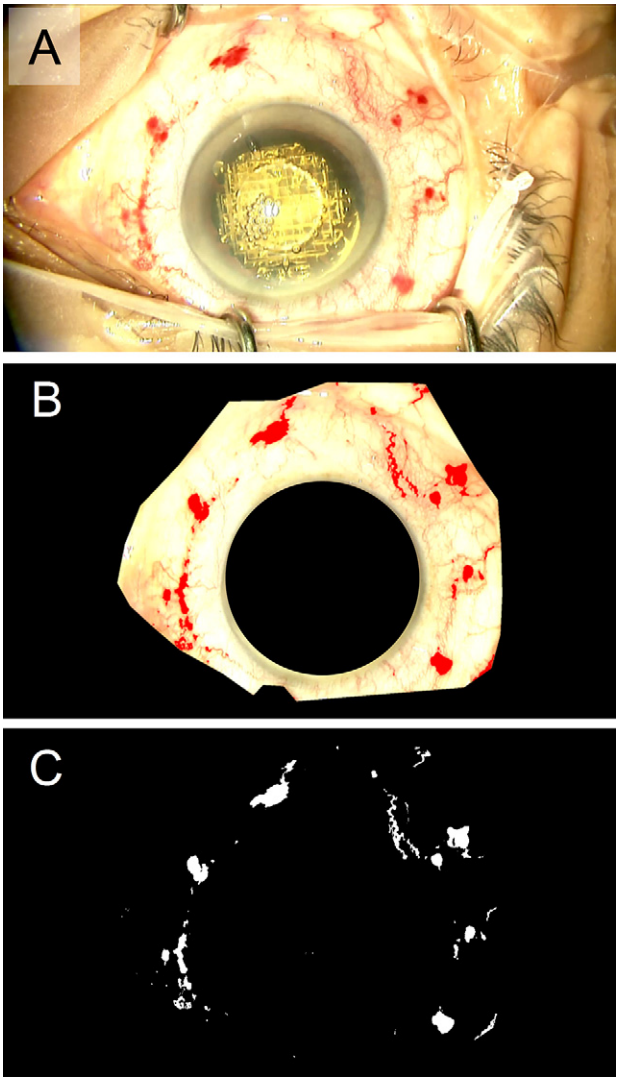

Figure 5. *A*: View of an eye under the operating microscope after laser surgery and before to completion of cataract surgery. *B*: The region of interest was identified by manual tracing of visible sclera and limbus and the total number of pixels in the outlined area calculated. *C*: The image was then filtered by color to produce a binary map discriminating the bright *red* from the background (*shown in white*).

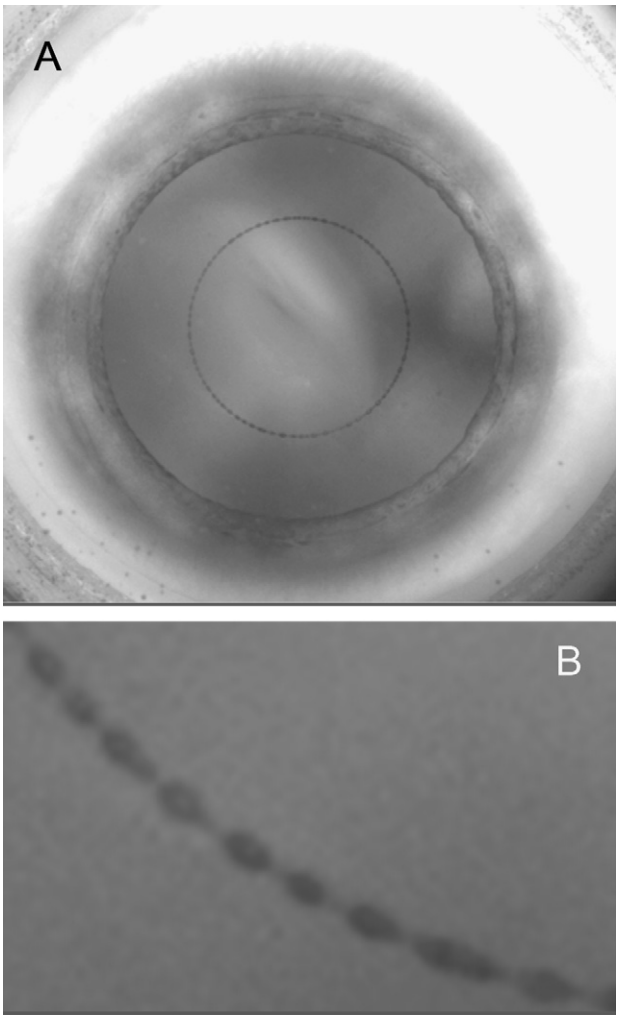

Figure 6. *A*: Typical appearance of an eye attached to the LOI interface. No folds are observed in the cornea with OCT or infrared video. *B*: Laser cut of the capsulotomy pattern appears continuous, with no skipped areas.

system (no folds). Wavefront error increased from 0.01 waves at the treatment wavelength to a sizable 0.94 waves, and Strehl ratio decreased from 1.0 to 0.2. The modeled geometry and this degradation affect on the beam irradiance pattern at focus are shown in Figure 7, *B*.

In Vitro Intraocular Pressure Measurement After Docking

Intraocular pressure in porcine and cadaver eyes increased linearly with the suction vacuum level for both interfaces, as shown in Figure 8. However, the IOP rise with the LOI system was much lower than with the CCL. For example, at suction vacuum of 500 mm Hg, the mean IOP rise with LOI was 16.6 mm Hg $\pm$ 1.8 (SD), while with CCL it was more than 4 times higher: 80.4 $\pm$ 10.4 mm Hg. To limit IOP rise, the CCL interface was applied under a suction vacuum of 150 mm Hg, resulting in an IOP rise of 32 mm Hg. The linear fitting lines for all 3 sets of measurements (porcine and cadaver) cross the y-axis above zero because application of vacuum initiates deformation of the eye to conform to the mechanical interface, resulting in a small nonlinear IOP rise.

Measurements of Eye Stability

The stability of the eye attached to the laser interface was assessed using analysis of the video frames

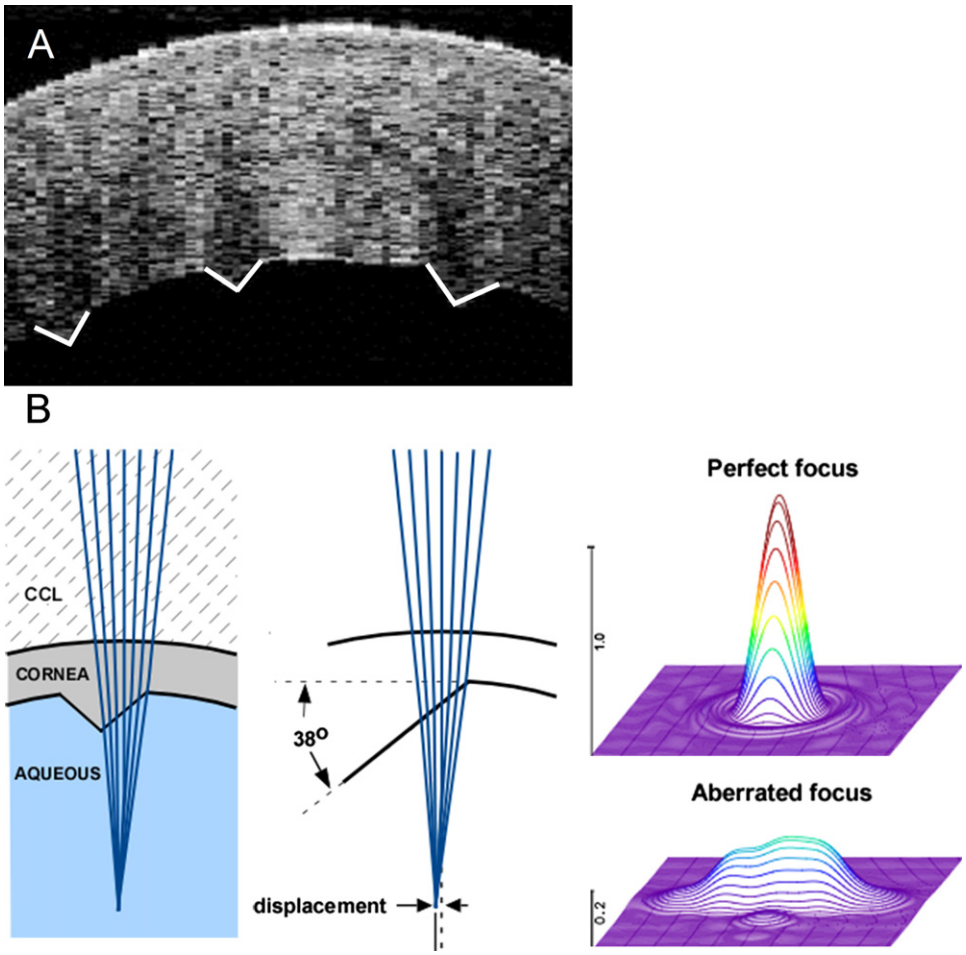

Figure 7. *A*: The OCT of a cornea attached to the CCL interface with 3 corneal folds on the posterior surface. *B*: The folds are modeled as wedges with 38-degree angles. Ray tracing of a laser beam converging into focus behind the wedge shows a beam shift and degradation of the focus (CCL = curved contact lens interface).

as a maximum drift during the time of observation. The suction vacuum of 150 mm Hg was used with CCL and 500 mm Hg was applied with LOI. Table 1 shows the results of these analyses.

Measurements of Subconjunctival Hemorrhage

Subconjunctival hemorrhaging was assessed as the ratio of the bleeding area to the visible area of the sclera. As described above, the area of bleeding was quantified using color filtering and thresholding (Figure 5). The mean hemorrhage area ratio was 0.14 ± 0.09 with CCL (n = 36) and 0.09 ± 0.07 with LOI (n = 35), showing a 36% reduction in subconjunctival hemorrhaging with LOI compared with that with CCL (plotted in Figure 9) ($P < .007$, Wilcoxon rank-sum test). Figure 9 shows the typical appearance of subconjunctival hemorrhaging after completion of laser surgery. The top row shows typical ring-like appearance of subconjunctival hemorrhaging with the CCL interface. The bottom row shows much less pronounced and more diffuse appearance of subconjunctival hemorrhaging, typical for the LOI.

DISCUSSION

The importance of achieving a complete laser capsulotomy cut cannot be understated. Capsule adherence could result in an unanticipated radial anterior capsule tear if the surgeon is unaware of its existence or if inappropriate direction of the force is applied when pulling away the excised tissue. Radial tears could compromise subsequent surgical steps and lead to more serious operative complications, such as zonular damage, posterior capsule rupture, and vitreous loss.

Corneal folds cause lateral shifts of the laser beam and degrade the quality of the focus for the imaging and the treatment beams. This in turn results in problems with identification of the correct location of target tissue structures and, in the case of laser capsulotomy, discontinuities of the laser cut. The best way to estimate the effect of corneal folds on laser beam energy is to calculate the Strehl ratio. The Strehl ratio represents the quality of the point-spread function at the image plane of an optical system and is defined as the ratio of the central beam irradiance at the focal point in the presence of aberration to the irradiance that would be obtained without aberration.[11] A perfect

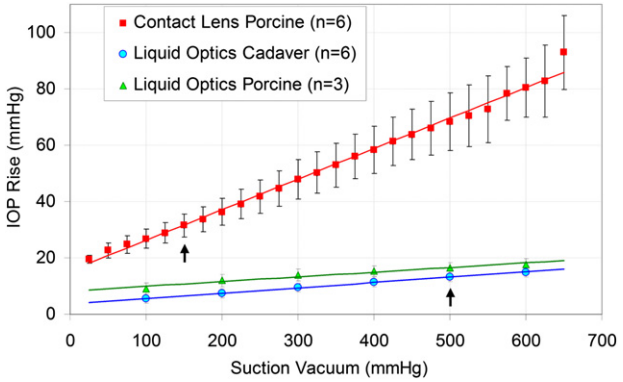

Figure 8. Rise of IOP with increasing vacuum for CCL and LOI interface devices measured ex vivo in porcine and human cadaver eyes. Vacuum levels used for human surgeries with the CCL (150 mm Hg) and LOI (500 mm Hg) are denoted by arrows (IOP = intraocular pressure).

optical system would have a Strehl ratio of 1.0. In the setting of corneal folds, the Strehl ratio is directly related to the amount of energy required for dielectric breakdown in the tissue. A decrease in laser irradiance at the focal point due to a Strehl ratio reduction from 1.0 to 0.2 corresponds to an approximately 5-fold increase in the dielectric breakdown threshold. Profiles of the actual corneal folds are more complex than the simple 2-sided wedge used in the optical model shown in Figure 7. As such, the calculated Strehl ratio from the modeling in Figure 7 probably underestimates the degree of beam distortion and decrease in laser irradiance at a focal point behind the corneal folds.

Decreasing laser irradiance at the focal point by a factor of 5, as simulated in the optical modeling, would strongly diminish or even completely prevent dielectric breakdown within the anterior capsule target tissue, resulting in the lack of cutting behind the folded areas. This problem could be overcome by increasing the pulse energy; however, this solution has numerous drawbacks. Outside the areas of corneal folds, high-energy explosions result in a rougher edge of the capsule cut and as a result, likely reduce the strength of the capsulotomy edge.[8] In addition, higher energy pulses applied to lens segmentation produce more residual gas trapped inside the lens. Large amounts of accumulated gas may lead to extensive expansion of the volume of the lens and capsular bag, potentially endangering the integrity of the latter.[12] Therefore, a beam-delivery approach such as the LOI, which does not produce corneal folds, allows the use of lower pulse energy, resulting in smoother and stronger capsulotomies and less gas accumulation in the lens.

A second limitation of the CCL is the difficulty of matching the eye's shape at the limbus, where the tissue radius of curvature rapidly transitions from the corneal radius averaging 7.8 mm, to the scleral radius

Table 1. Maximum eye shift (95% percentile) observed under CCL and LOI during the 3 time intervals studied.

	Eye Drift (μm)	
Duration	CCL (n = 24)	LOI (n = 32)
1.5 s	50	20
20 s	160	100
2 mins	360	100

CCL = curved contact lens interface; LOI = liquid optical immersion interface

approximating 12.0 mm. The challenge of matching such a complex shape is further aggravated by great anatomic variability among patients. To provide a tight seal against the ocular surface using a contact lens while accounting for variations in limbal curvature and corneal diameter, the contact lens is typically kept smaller than the limbus diameter. In our case, the edge diameter was limited to 12.0 mm while the clear aperture was limited to 10.8 mm. This places restrictions on laser applications at the periphery, such as limbal relaxing incisions and clear cataract incisions.

Because the LOI comes in mechanical contact only with sclera and its overlying conjunctiva, wide disparities in corneal and/or limbal anatomy can be accommodated and the clear aperture can be extended beyond the limbus. A larger clear aperture makes it easier for the surgeon to perform docking and increases the odds that the patient interface will be well centered over the cornea to allow accurate incision placement. The only width-limiting factor with the LOI is the maximum opening of the eyelids to accommodate the suction ring attached to the eye. In our design, for example, the clear aperture diameter on the cornea was 14.5 mm and the outer diameter of the suction ring was 21.5 mm. This larger aperture requirement may prove to be an ergonomic issue for smaller orbits such as those routinely seen in Asian populations, and a smaller diameter LOI is currently under development by our group to address this issue.

Another potential drawback of the LOI is the need to precisely identify the anterior corneal surface necessary for placement of the corneal cuts. Unlike the CCL, which forces the cornea against the contact lens surface and thereby provides easy identification of the corneal epithelial surface, the LOI requires sophisticated imaging modalities to ensure precise mapping.

Deformation of the globe against a solid surface that does not perfectly match the natural eye shape results in elevation of the IOP. With a CCL interface, the vacuum-induced IOP rise was, on average, approximately 32 mm Hg. This is much lower than the maximum values (80 to 90 mm Hg) reported with applanating refractive surgical laser systems.[2–4] As a consequence,

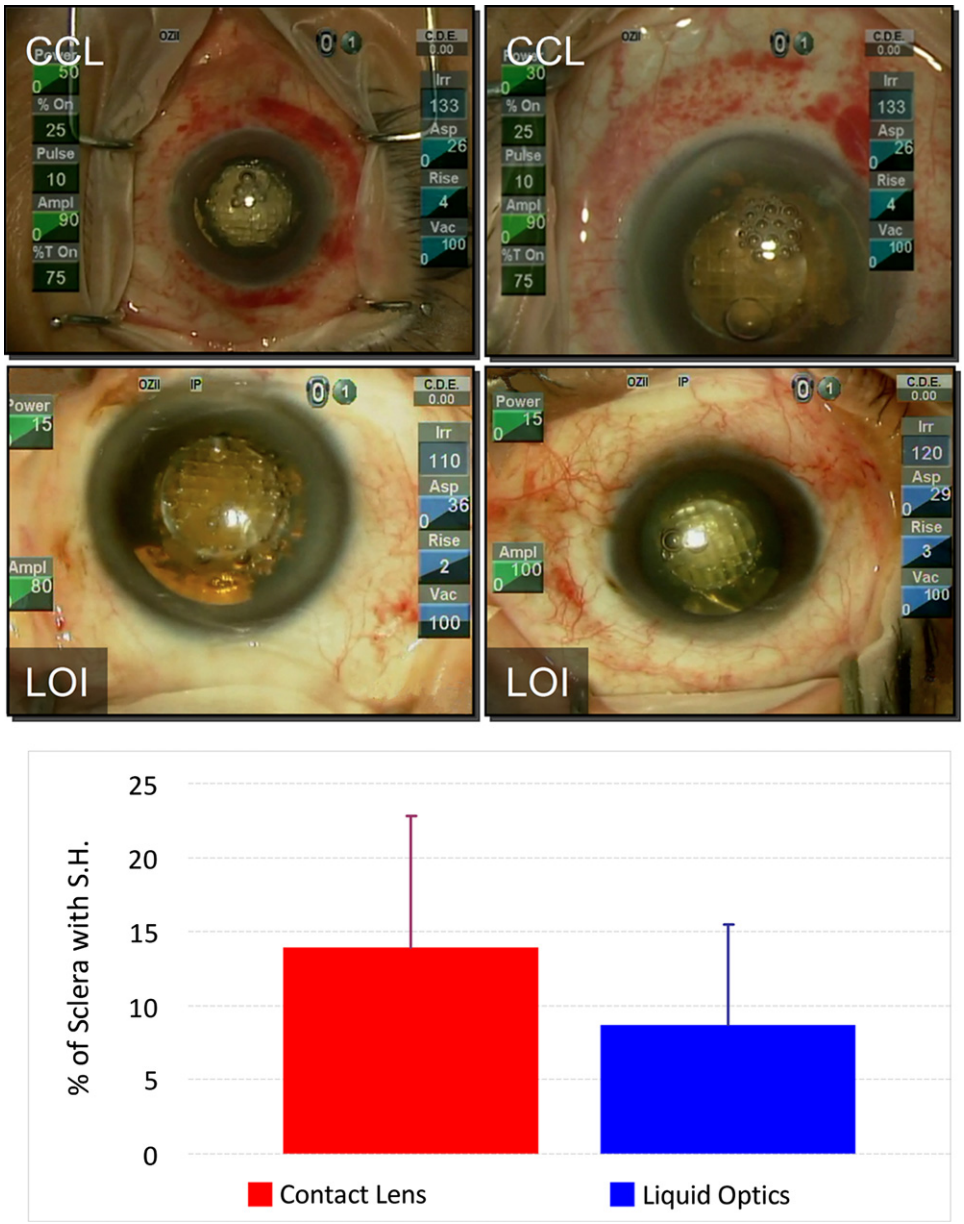

Figure 9. Typical appearance of subconjunctival hemorrhage as observed through a surgical microscope prior to cataract surgery. *Top row*: Curved contact lens interface. *Second row*: Liquid optics immersion interface. *Bottom*: Relative area of subconjunctival hemorrhage (%) with CCL and LOI interface (CCL = curved contact lens interface; LOI = liquid optical immersion interface; S.H. = subconjunctival hemorrhage).

systems that use an applanating interface are contraindicated for patients with glaucoma. With the liquid interface, the eye was much less deformed and the vacuum-induced IOP rise was limited on average to 18 mm Hg. At this lower IOP level, even if the vacuum is applied for several minutes, it is unlikely to cause damage to the optic nerve microcirculation or the retinal vasculature. A recent in vivo human study using the identical LOI design[13] produced very similar results to these ex vivo measurements, which corroborates the validity of this model, at least for the LOI subgroup.

Ocular motility under dock was studied because of an initial concern that the reduced area of mechanical contact between the LOI and the ocular surface (versus the CCL) might result in decreased stability of the globe. The interval of 1.5 seconds was chosen because it closely approximates the actual time needed to create an anterior capsulotomy with commercially available femtosecond lasers. With a properly designed suction ring, the mechanical stability of the eye did not deteriorate but actually improved versus the CCL.

Even with the higher vacuum level applied to achieve stable docking with a LOI, the suction ring produced less subconjunctival hemorrhaging than with the CCL interface. Although subconjunctival hemorrhaging typically disappears within the first 2 weeks after surgery,[6] mitigation of this problem is an important aesthetic benefit for many patients. This is especially important in individuals who are

taking anticoagulant medications (eg, aspirin, clopidogrel bisulfate, warfarin).

In conclusion, a CCL used with a femtosecond laser system caused significant folds of the posterior corneal surface with resultant degradation of the treatment laser beam's focal point, often resulting in an incomplete capsulotomy cut. An LOI resolved this problem and allowed complete capsulotomy in all cases. Despite having reduced direct contact area with the eye, the liquid interface improved globe stability during treatment and reduced the IOP elevation compared with that with the curved contact lens in an ex vivo porcine and cadaver eye model system. With the LOI, the lateral field of view in the eye could be increased and the amount of subconjunctival hemorrhage after surgery was significantly reduced.

Although this study compares the 2 current types of optomechanical interface, there is no doubt that this field will continue to evolve and new designs of flexible interfaces will be introduced and perfected over time. As the new systems become available, it will be important to quantify and compare the extent of corneal folding, the degree of IOP elevation, and the level of stability of the eye during imaging and subsequent laser treatment.

WHAT WAS KNOWN

- Corneal folds are a well-known byproduct of corneal applanation during femtosecond laser surgery, but their optical impact on laser cataract surgery was uncertain.
- Intraocular pressure elevation, globe stability, and a clear optical path are affected by the design of the patient interface, but the relative advantages and disadvantages of different interface designs for laser cataract surgery have not been shown.
- Conjunctival hemorrhage is common after femtosecond laser surgery with contact corneal applanation interfaces.

WHAT THIS PAPER ADDS

- Corneal folds during laser-assisted cataract surgery caused incomplete capsulotomies. Optical modeling suggests that this problem can be mitigated, but only if laser pulse energy is significantly increased.
- A liquid immersion interface offers numerous advantages over corneal contact applanation. Corneal folds do not occur (avoiding a major cause of incomplete capsulotomy), globe stability is improved, there is less IOP rise, and there are reduced amounts of postoperative subconjunctival hemorrhage.

REFERENCES

1. Talamo JH, Meltzer J, Gardner J. Reproducibility of flap thickness with IntraLase FS and Moria LSK-1 and M2 microkeratomes. J Refract Surg 2006; 22:556–561
2. Bissen-Miyajima H, Suzuki S, Ohashi Y, Minami K. Experimental observation of intraocular pressure changes during microkeratome suctioning in laser in situ keratomileusis. J Cataract Refract Surg 2005; 31:590–594
3. Bradley JC, McCartney DL, Craenen GA. Continuous intraocular pressure recordings during lamellar microkeratotomy of enucleated human eyes. J Cataract Refract Surg 2007; 33:869–872
4. Kasetsuwan N, Pangilinan RT, Moreira LL, DiMartino DS, Shah SS, Schallhorn SC, McDonnell PJ. Real time intraocular pressure and lamellar corneal flap thickness in keratomileusis. Cornea 2001; 20:41–44
5. Conway ML, Wevill M, Benavente-Perez A, Hosking SL. Ocular blood-flow hemodynamics before and after application of a laser in situ keratomileusis ring. J Cataract Refract Surg 2010; 36:268–272
6. Kobayashi H. Evaluation of the need to discontinue antiplatelet and anticoagulant medications before cataract surgery. J Cataract Refract Surg 2010; 36:1115–1119
7. Palanker DV, Blumenkranz MS, Andersen D, Wiltberger M, Marcellino G, Gooding P, Angeley D, Schuele G, Woodley B, Simoneau M, Friedman NJ, Seibel B, Batlle J, Feliz R, Talamo J, Culbertson W. Femtosecond laser-assisted cataract surgery with integrated optical coherence tomography. Sci Transl Med 2010; (2): 58ra85. Available at: http://www.stanford.edu/~palanker/publications/fs_laser_cataract.pdf. Accessed January 17, 2013
8. Friedman NJ, Palanker DV, Schuele G, Andersen D, Marcellino G, Seibel BS, Batlle J, Feliz R, Talamo JH, Blumenkranz MS, Culbertson WW. Femtosecond laser capsulotomy. J Cataract Refract Surg 2011; 37:1189–1198
9. Chylack LT Jr, Wolfe JK, Singer DM, Leske MC, Bullimore MA, Bailey IL, Friend J, McCarthy D, Wu S-Y, for the Longitudinal Study of Cataract Study Group. The Lens Opacities Classification System III. Arch Ophthalmol 1993; 111:831–836
10. Aslanides IM, Tsiklis NS, Ozkilic E, Coskunseven E, Pallikaris IG, Jankov MR. The effect of topical apraclonidine on subconjunctival hemorrhage and flap adherence in LASIK patients. J Refract Surg 2006; 22:585–588
11. Lombardo M, Lombardo G. Wave aberration of human eyes and new descriptors of image optical quality and visual performance. J Cataract Refract Surg 2010; 36:313–331
12. Roberts TV, Sutton G, Lawless MA, Jindal-Bali S, Hodge C. Capsular block syndrome associated with femtosecond laser-assisted cataract surgery. J Cataract Refract Surg 2011; 37:2068–2070
13. Schultz T, Conrad-Hengerer I, Hengerer FH, Dick HB. Intraocular pressure variation during femtosecond laser–assisted cataract surgery using a fluid-filled interface. J Cataract Refract Surg 2013; 39:22–27

First author:
Jonathan H. Talamo, MD

Private practice, Waltham, Massachusetts, USA